THERMAL FATIGUE PROPERTIES OF LASER TREATED STEELS

S.N. Aqida[1], F. Calosso[2], D. Brabazon[1*], S. Naher[1] and M. Rosso[2]

[1]Materials Processing Research Centre, Dublin City University, Ireland
[2] Faculty of Engineering, Politecnico Di Torino, Italy
* Dermot Brabazon: Dublin City University, Dublin 9, +35317008213, +35317005345, dermot.brabazon@dcu.ie

ABSTRACT: This paper presents the thermal fatigue resistance of laser treated steels. The C40 and AISI H13 steels were machined into a geometry which allowed thermal gradients on the inner and outer surface during testing. A CO_2 laser system was used with a focused spot size of 0.09 mm on the sample surface. The laser peak power and pulse repetition frequency (PRF) range were set to 760 and 1515 W, and 2900 to 3500 Hz respectively. The thermal fatigue machine used consists of Nabertherm model cylindrical high temperature furnace with digital control panel, controlled temperature quenching system, and pneumatics control sample movement mechanism. The thermal fatigue test involved immersion of samples into molten aluminium, and quenched in ionised water emulsion at 17 °C temperature. The quenching system equipped with thermocouple to control the water temperature. Testing was done at a total of 1,750 number of cycles. Internal surface cooling was controlled by water inlet and outlet tubes. Samples were cleaned using NaOH solution after thermal fatigue testing to remove oxides on the surface. The solution temperature and magnetic stirrer speed were set to 100 °C and 4.5 rpm respectively. Samples were characterised using scanning electron microscope (SEM), energy discharge x-ray spectroscopy (EDXS) and 2D stylus profilometer. Presence of different phases on the sample surface were analysed from back-scattered detector micrographs. Heat checks were observed on laser glazed surface at several regions. Carbides and oxides elements were detected on the sample surface after the thermal fatigue test. The relationship between surface roughness of laser treated surface and thermal fatigue behaviour was investigated.
KEYWORDS: Laser treatment, thermal fatigue, SEM, surface roughness.

1 INTRODUCTION

In semi-solid forming, sustaining dies life by surface treatment and coatings have been extensively done for thermal barrier. Challenging requirement of effective coating caused surface treatment more favourable to protect dies from premature failure. The thermal fatigue premature failure in semi-solid forming involves dies exposure to molten non-ferrous metal at high temperature for thousands of cycles. Thermal stresses from temperature gradients between sample outer and inner diameter initiate cracks as the material strength decrease at higher temperatures [1, 2].

The laser beam can be utilised for AISI H13 surface treatment to enhance the mechanical properties, it is possible to modify the structural steels or alloy steels [3-5]. By laser processing, the steel surface was rapidly melted (above austenite temperature of 1727 K) and rapidly quenched. The treated layer exhibit high hardness due to formation of finer grains, secondary carbide and hard non-equilibrium microstructures that are intimately bonded to the substrate and the modified region itself [6, 7].

In this study C40 structural steel and H13 tool steel were laser treated to investigate their thermal fatigue properties in the semi-solid forming applications. The thermal fatigue

properties were examined through customized fatigue testing while characterisation was made using 2D profilometer and metallographic study.

2 EXPERIMENTAL

Two types of steel investigated are C40 and AISI H13 with chemical composition given in Table 1. The sample geometry was machined to an outer diameter of 33 mm, inner diameter of 22 mm and 55 mm length to fit the fatigue testing machine as shown in Figure 1. The sample longitudinal surface was treated by rotating and linearly translating it perpendicular to the laser firing direction. Each sample surface was processed with four parameter settings as given in Table 2.

Table 1 Chemical composition of AISI H13 and C40 steels.

Elements (wt %)											
Material	C	Mn	Si	Cr	Ni	Mo	V	Cu	P	S	Fe
H13	0.32-0.45	0.20-0.50	0.80-1.20	4.75-5.50	0.30	1.10-1.75	0.80-1.20	0.25	0.03	0.03	Bal.
C40	0.37-0.44	0.50-0.80	≤0.40	≤0.40	≤0.40	≤0.10	-	-	≤0.035	≤0.035	Bal.

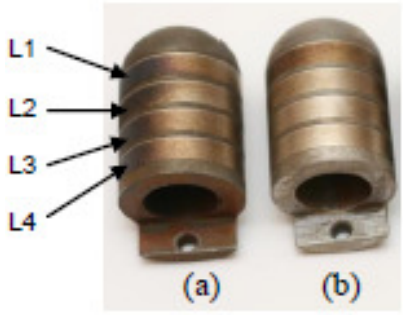

Figure 1 Laser treated (a) C40 and (b) AISI H13 samples.

A Rofin DC-015 diffusion-cooled CO2 slab laser system with 10.6 μm wavelength was used. The laser beam was focused to a spot size of 0.09 mm onto the sample surface. The process parameters and sample translation speed are given in Table 2. The laser spot traverse speed was calculated based on the PRF to allow uniform distance between the spots. The traverse speeds were at 261 mm/s and 315 mm/s. Argon gas was used during the process at 1 bar pressure. The thermal fatigue testing machine consists of Nabertherm model cylindrical high temperature furnace with digital control panel, controlled temperature quenching system, and pneumatics control sample movement mechanism as shown in Figure 2. Samples were immersed into molten aluminium alloy at 850 °C and quenched in ionised water emulsion at 17 °C temperature for 4 seconds each to imitate the semi-solid forming process. The heating and quenching cycle was repeated for 1,750 times with a single cycle required 28 seconds to complete. Samples were cleaned using NaOH solution after thermal fatigue testing to remove oxides on the surface. The solution temperature and stirring speed were set to 100 °C and 4.5 rpm respectively.

Characterisation of thermal fatigued samples was done using EVO-LS15 SEM. EDXS was also done using Oxford equipment to indicate presence of carbides and oxides on the sample surface. Surface roughness measurement was done using TR200 measuring system integrated with software to measure the surface profile before thermal fatigue testing.

Table 2 Laser treatment parameters.

Parameter	Peak power (W)	PRF (Hz)	Pulse width (ms)	Chuck speed (rpm)	Traverse speed (mm/s)
L1	1515	2900	0.062	151	261
L2	760	2900	0.125	151	261
L3	1515	3500	0.052	182	315
L4	760	3500	0.103	182	315

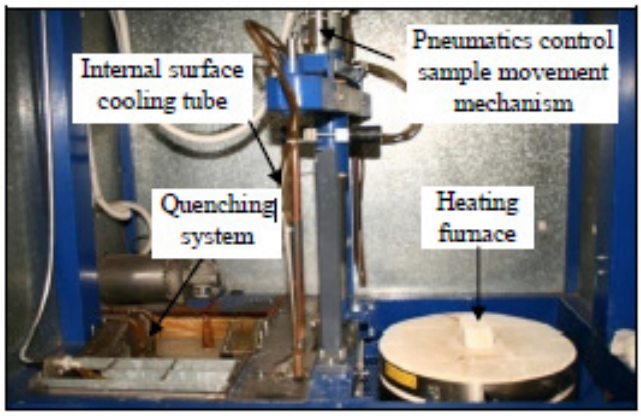

Figure 2 Thermal fatigue testing system

3 RESULTS

The laser treatment parameters were set at 2900 Hz and 3500 Hz in order to gain pulse energy of 0.095 J and 0.078 J respectively. Table 3 shows the resulting surface roughness of C40 and AISI H13 steel after laser treated at different pulse energy and peak power. At 0.078 J pulse energy, the surface roughness measured was lower than samples treated at 0.095 J. By setting a low peak power of 760 W during 0.095 J and 0.078 J pulse energy, both C40 and H13 steels surface roughness increased.

Table 3 Surface roughness of laser treated steels.

Parameter	Pulse energy (J)	Range of surface roughness (μm)	
		C40	AISI H13
L1	0.095	3.23- 3.64	3.10 - 3.61
L2	0.095	8.26 - 8.85	7.79 - 7.99
L3	0.078	2.35 - 2.61	2.25 - 2.51
L4	0.078	7.36 - 8.25	4.34 - 7.35

Figure 3 (a) to (d) shows the SEM back scattered micrographs of the laser treated H13 surface. Figure 3 (a) to (c) shows uniform overlap surface morphology developed on the melted surface of samples treated by parameter L1 and L3. A significant correlation between surface roughness measurement in Table 3 and the treated H13 surface morphology at 1515 W peak power is shown by Figure 3 (a) and (c). Figure 3 (b) and (d) show the micrographs of sample surface treated at 760 W. Overlaps in these samples are irregular while over-melted surface and mount up melt pool regions are seen in Figure 3 (b).

The resulting surface morphology of H13 samples after thermal fatigue is given by micrographs in Figure 3(e) to (h). The back-scattered detector micrographs show presence of different phases on the sample surface. Dark regions on the thermal fatigue H13 surface were detected by EDXS as the substrate with high content of carbon and oxygen elements. Distribution of dark regions in Figure 3 (e) and (h) were observed in between the overlaps which prone to entrap the impurities during testing. At surface roughness range of 4.34 to 7.99 µm, more oxides and carbon were observed as given in Figure 3 (f) and (h).

However, surface treated by parameter L3 in Figure 3 (g) indicates a 'clean' surface after thermal fatigue. The laser treated C40 surface depicts a similar behaviour towards thermal fatigue. In Figure 4 (b) and (d), oxide and carbon entrapped excessively. In micrograph of Figure 4 (c), soldering occurred in C40 sample treated by parameter L3. Among the laser treatment settings, parameter L1 caused heat checks and cracks on both H13 and C40 samples. Using higher magnification, heat checks were observed on laser treated surface of H13 at several regions as shown in Figure 5 (a), while cracks on C40 surface were pointed in Figure 5 (b).

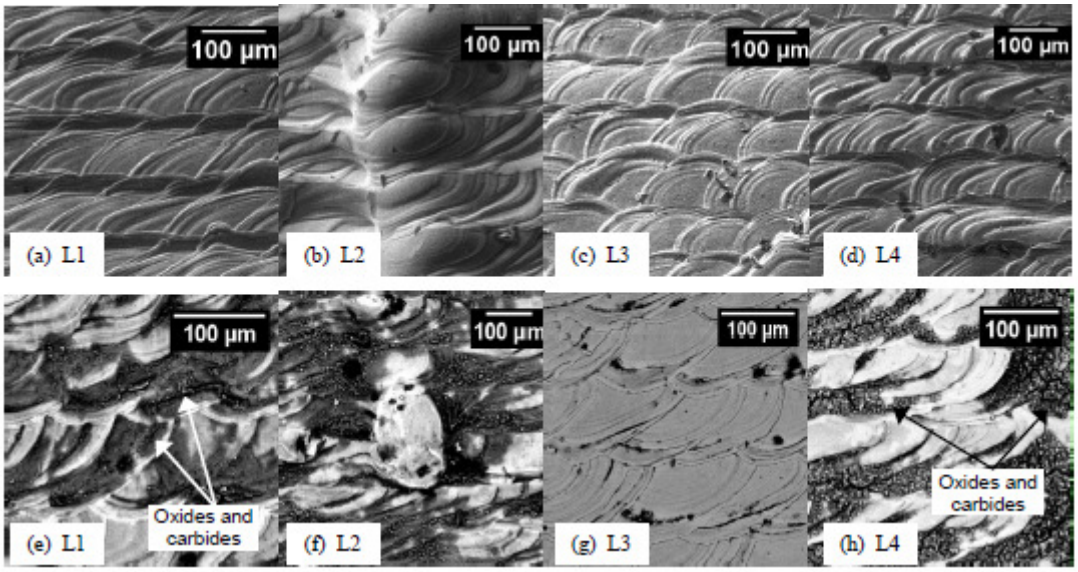

Figure 3 SEM micrographs of laser treated AISI H13 steel before (a) to (d), and after (e) to (h) thermal fatigue testing.

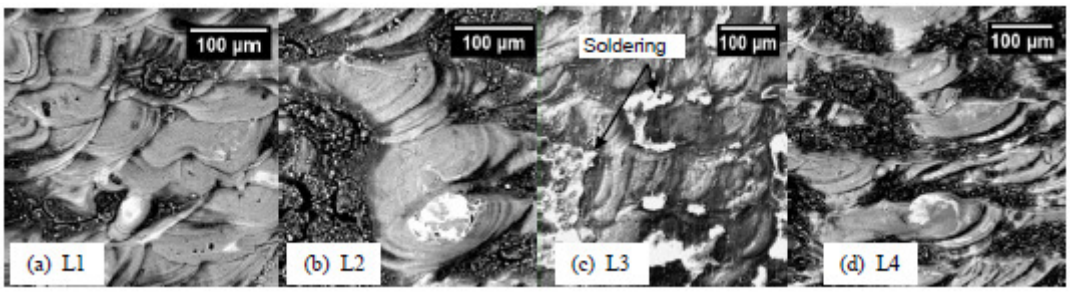

Figure 4 SEM micrographs of laser treated C40 steel after thermal fatigue test at L1, L2, L3 and L4 parameter.

4 DISCUSSION

Low PRF of 2900 Hz produces high pulse energy which developing heat sink on the laser irradiated surface. Hence, longer pulse width of 0.125 ms caused over-melted surface which resulted in high surface roughness. Whereas, short pulse width of 0.052 ms produced uniform overlaps without affecting the surface roughness noticeably.

Oxygen and carbon elements were introduced during sample immersion into high temperature molten aluminium, as the testing system was not vacuum. At high temperature, iron oxides easily formed while carbon impurities were resourced from the molten aluminium. The surface roughness on the treated surface depends on the efficiency of overlaps. High surface roughness with irregular overlaps possibly initiated cracks formation due to accumulated oxides and carbides on the surface. Low surface roughness reduced the possibility of molten aluminium entrapment during immersion. Soldering effect occurred in C40 steel while none visible on H13 surface. This is due to H13 steel contains higher content of molybdenum than C40 which provides soldering resistance [8]. The number of cycles tested on the samples was not effectively sufficient to produce noticeable cracks, craters or heat checks. However, premature failure occurred on C40 and H13 samples treated at parameter L1 due to high stress development on the surface during laser treatment. The incubated thermal stress from high pulse energy and power density resulted in premature failure when further applied with more thermal stresses from thermal fatigue.

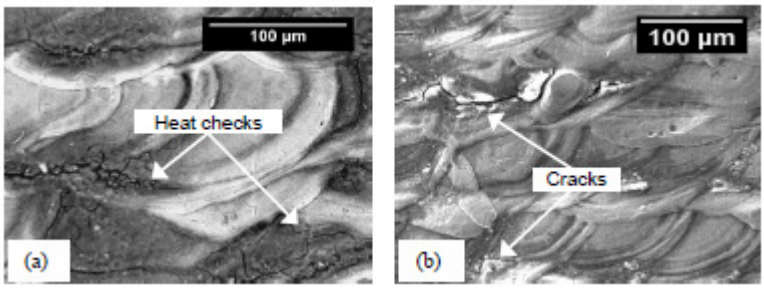

Figure 5 Heat checks and cracks in laser treated (a) AISI H13 and (b) C40 samples due to thermal fatigue.

5 CONCLUSION

A ‘clean’ surface was observed on H13 sample treated using peak power of 1515 W and 0.078 J pulse energy. At the same parameter setting, C40 sample experienced soldering effect due to thermal fatigue. Higher content of molybdenum in H13 increases the soldering resistance. Premature failure like heat checks and cracks occurred on samples treated at high peak power and pulse energy of 1515 W and 0.095 J respectively. High surface roughness of laser treated surface entrapped oxides and carbides which possibly initiates the thermal fatigue failure. Cracks and heat checks occurred on the carbides affected regions and soldered surface. The findings in this study are significant to consider the laser treatment parameter settings to enhance the thermal fatigue properties in semi-solid processing.

ACKNOWLEDGEMENT

The authors would also like to acknowledge the support from the Ministry of Higher Education, Malaysia and COST Action 541 for funding this work.

REFERENCES

[1] D. Klobcar, J. Tusek and B. Taljat. Thermal fatigue of materials for die-casting tooling. Mater. Sci. Eng., A 472:198–207, 2008.

[2] M. Pellizzari, A. Molinari and G. Straffelini. Thermal fatigue resistance of gas and plasma nitrided 41CrAlMo7 steel. Mater. Sci. Eng., A352:186-194, 2003.
[3] S. N. Aqida, M. Maurel, D. Brabazon, S. Naher and M. Rosso. Thermal stability of laser treated die material for semi-solid metal forming. Int. J Mater Form., Vol. 2 Suppl 1:761–764, 2009.
[4] D. Brabazon, S. Naher and P. Biggs, Laser surface modification of tool steel for semi-solid steel forming, Solid State Phenomena, 141-143:255-260, 2008.
[5] D. Brabazon, S. Naher, and P. Biggs. Glazing of tool dies for semi-solid steel forming. Int. J. Mater. Form. DOI 10.1007/s12289-008-0, Springer/ESAFORM 2008.
[6] R.J. DiMelfi, P.G. Sanders, B. Hunter, J.A. Eastman, K.J. Sawley, K.H. Leong, and J.M. Kramer, Mitigation of subsurface crack propagation in railroad rails by laser surface modification. Surf. Coat. Tech., 106:30-43, 1998
[7] SeDao, S., Hua, M., Shao, T.M., Tam, H.Y., Surface modification of DF-2 tool steel under the scan of a YAG laser in continuously moving mode. J. Mater. Process. Tech., doi:10.1016/j.jmatprotec.2008.10.058, 2009.
[8] Z. Hanlian, G. Jingjie, J. Jun, Experimental study and theoretical analysis on die soldering in aluminum die casting. J. Mater. Process. Tech., 123: 229–235, 2000